The Meteoritical Society

Meteoritics & Planetary Science 43, Nr 7, 1137–1146 (2008)
Abstract available online at http://meteoritics.org

Crystallization experiments on a Gusev Adirondack basalt composition

J. FILIBERTO[1*], A. H. TREIMAN[1], and L. LE[2]

[1]Lunar and Planetary Institute, 3600 Bay Area Blvd., Houston, Texas 77058, USA
[2] Jacobs Sverdrup Engineering and Science, Houston, Texas 77058, USA
[*]Corresponding author. E-mail: filiberto@lpi.usra.edu

(Received 15 June 2007; revision accepted 21 December 2007)

Abstract–Until recently, the SNC meteorites represented the only source of information about the chemistry and petrology of the Martian surface and mantle. The Mars Exploration Rovers have now analyzed rocks on the Martian surface, giving additional insight into the petrology and geochemistry of the planet. The Adirondack basalts, analyzed by the MER Spirit in Gusev crater, are olivine-phyric basaltic rocks which have been suggested to represent liquids, and might therefore provide new insights into the chemistry of the Martian mantle. Experiments have been conducted on a synthetic Humphrey composition at upper mantle and crustal conditions to investigate whether this composition might represent a primary mantle-derived melt. The Humphrey composition is multiply saturated at 12.5 kbar and 1375 °C with olivine and pigeonite; a primary anhydrous melt derived from a "chondritic" mantle would be expected to be saturated in orthopyroxene, not pigeonite. In addition, the olivine and pigeonite present at the multiple saturation are too ferroan to have been from a Martian mantle as is understood now. Therefore, it seems likely that the Humphrey composition does not represent a primary anhydrous melt from the Martian mantle, but was affected by mineral/melt fractionations at lower (crustal) pressures.

INTRODUCTION

Until recently, the Martian meteorites (SNCs) represented the only sources of information about igneous processes on the Martian surface (McSween 2002). Many experiments have been conducted on Martian meteorite compositions to investigate their parental liquid compositions and crystallization sequences, and therefore provide information about the mantle that produced such rocks (e.g., McCoy and Lofgren 1999; Dann et al. 2001; Musselwhite et al. 2006; Nekvasil et al. 2007a; Filiberto 2008). The Martian meteorites (except Allan Hills [ALH] 84001) are relatively young (1.3–0.17 Ga; e.g., Jones 1986, 2007b; Nyquist et al. 2001; Treiman 2005), so experiments on these rocks provide information about young magmatism and the present Martian mantle. Recently, however, the Mars Exploration Rover Spirit analyzed basaltic rocks on the surface of Mars that have been suggested to be 3.65 Ga old (Greeley et al. 2005), and thus may provide data about the ancient geochemistry of the Martian mantle.

Among the rocks analyzed on Mars by the Spirit rover are Adirondack-class basalts—fine-grained rocks of basaltic compositions, with megacrysts interpreted as ferroan olivine (~$Fo_{60 \pm 10}$) by Mössbauer (Morris et al. 2004; Morris personal communication), and with irregular vesicles and vugs (Morris et al. 2004; Gellert et al. 2006; McSween et al. 2006). The Adirondack-class rocks are interpreted as fragments of basalt lava flows, probably representing basaltic magma (not crystal cumulates and not affected by chemical alteration) (McSween et al. 2006; Monders et al. 2007). If the Adirondack-class rock compositions do represent magma compositions, experiments on their melting and crystallization will yield useful information about ancient igneous processes on Mars, and possibly show whether these compositions represent primary mantle derived melts.

A basaltic liquid composition may represent a primary mantle melt if it is co-saturated with expected mantle minerals (olivine, orthopyroxene, spinel, etc.) of likely chemical compositions at a reasonable mantle pressure and temperature (e.g., Asimow and Longhi 2004). Experimental studies testing a possible mantle origin have been conducted on the composition of the Martian meteorite Yamato (Y-) 980459 (anhydrous, Musselwhite et al. 2006), and on an average Adirondack-class basaltic composition (hydrous, with 0.8 wt% water, Monders et al. 2007). Both sets of experiments produced olivine and orthopyroxene on the liquidus at their respective multiple saturation points, suggesting that both rocks could represent primary mantle melts. However, the

Table 1. Starting composition compared with published results (calculated Cr-free and normalized to 100%).

wt%	Gellert et al. (2006)	McSween et al. (2006)	Experimental glass composition
SiO_2	46.96	46.49	45.99
TiO_2	0.56	0.59	0.56
Al_2O_3	10.93	10.55	10.89
FeO_T	19.23	18.95	20.01
MnO	0.42	0.43	0.42
MgO	10.65	10.82	10.89
CaO	8.02	8.26	8.12
Na_2O	2.56	2.38	2.44
K_2O	0.10	0.09	0.10
P_2O_5	0.57	0.60	0.58
FeS	0.00	0.84	0.00
Total	100.00	100.00	100.00

FeO_T = total iron (Fe_2O_3 + FeO).

mineral compositions (i.e., Fo_{84} for Y-980459 versus Fo_{73} for Adirondack-class basalt) are rather different, suggesting dissimilar mantle source regions for each rock; the Adirondack-class magma would have come from a much more evolved mantle composition (Fe-rich). A direct comparison of these two studies is complicated because the Y-980459 study was conducted without water, while the Humphrey experiments contained 0.8 wt% water; dissolved water can have large effects on phase equilibria and liquidus temperatures (e.g., Zeng et al. 1999; Danyushevsky 2001; Nekvasil et al. 2004; Médard and Grove 2006, 2007). Since the Martian meteorites do not contain much water (e.g., Watson et al. 1994; Leshin et al. 1996; Dyar et al. 2004; Jones 2004, 2007a) and because they are our only samples of Martian basalts, it is reasonable to conduct experiments with very low water contents (i.e., relatively anhydrous).

To investigate whether the Adirondack class basalts are primary anhydrous mantle derived liquids, a suite of near-liquidus experiments have been conducted from 1 bar to 15.7 kbar on one of the analyzed Adirondack-class basalt compositions, the Humphrey rock, in a similar manner to previous experimental studies (Musselwhite et al. 2006; Monders et al. 2007). Humphrey was chosen for this study because it is appears to be the least altered of the Adirondack class basalts (McSween et al. 2006) and experiments can be compared with the previous hydrous study (Monders et al. 2007).

EXPERIMENTAL TECHNIQUE

A synthetic powdered starting material of the Humphrey composition was made from a homogenized mixture of element oxides. The starting composition for this study was made Cr-free to avoid the fO_2 effects on chromite stability (Onuma and Tohara 1983; Monders et al. 2007). The powder was then melted at 1400 °C at 1 atm to produce a homogeneous anhydrous glass (Table 1). The glass was ground to powder, remixed to ensure homogeneity, and stored in a desiccator to ensure that it remained anhydrous. High pressure experiments were conducted near the liquidus (1400–1300 °C) at mantle pressures (4–16 kbar). 1 bar experiments were conducted from near the liquidus through 16% crystallization (1300–1200 °C).

High-Pressure Experiments

High-pressure experiments were conducted in a QuickPress® piston-cylinder apparatus in the laboratories of the ARES division, Johnson Space Center. After loading the powder into a graphite capsule, both were dried at 150 °C for at least 12 h to ensure that they remained volatile free. The sample capsule and graphite furnace were held in $BaCO_3$ sleeves and crushable MgO spacers. Temperature was measured using a W5Re/W25Re thermocouple placed in an indentation in the graphite sample capsule. Pressures in these experiments ranged from 4 kbar to 16 kbar nominal, as measured on a Heise gauge. Based on the location of the diopside melting curve, pressures were corrected by –0.3 kbar at 7 kbar and above nominal pressure and –2.0 kbar correction at 4 kbar nominal pressure (see Appendix for diopside melting calibration experiments). The oxygen fugacity, fO_2, of our experiments has not been directly measured. However, the graphite capsules constrain the fO_2 of the assemblage, at elevated pressures, to ~1.5 to 3.5 log units below the FMQ oxygen buffer (Holloway et al. 1992).

Experiments were conducted using a piston-out procedure—the experiment was pressurized cold to 2 kbar above the experimental pressure, brought to melting temperature, and then brought down to the final pressure. Samples were melted for 30 min above the liquidus temperature, rapidly cooled to the final crystallization temperature where they remained for 1–4 h (longer times were for lower temperatures), and finally quenched at pressure. This technique was employed in order to mimic natural magmatic conditions where crystals form directly from a molten liquid, rather than synthesis techniques of going directly to the crystallization temperature where crystals form from the powder. Capsules remained intact during the experiments (no cracks in the capsule walls) and no barium contamination from the pressure sleeve occurred.

1 bar Experiments

One bar experiments were conducted in a 1 atm Deltech gas mixing furnace in the laboratories of the ARES division, Johnson Space Center. The oxygen fugacity was controlled mixing CO-CO_2 gas with a desired fO_2 at or near the fayalite-magnetite-quartz (FMQ) buffer and at or near 1 log unit below the iron-wüstite (IW) buffer. Oxygen fugacity was measured in a reference furnace through which exhaust gases from the experimental furnace were passed (Jurewicz et al.

1993). Temperature was measured using a $Pt_{94}Rh_6$-$Pt_{70}Rh_{30}$ thermocouple calibrated against the melting point of Au. For experiments at FMQ, 125 mg of the Humphrey synthetic mix was pressed into a pellet and sintered onto a Pt loop. For experiments conducted at IW-1 the powder was mixed with poly-vinyl alcohol (PVA) and pasted onto a Re-wire loop to prevent Fe loss to the Pt wire. Experiments conducted at FMQ were melted for 2 days to ensure homogeneity and equilibrium with the oxygen fugacity, crystallized for 2 days to ensure fO_2 and mineral equilibrium, and then air quenched. The experiments conducted at IW-1 were melted for 1 day and crystallized for 1 day to reduce the volatilization of Na_2O. All experimentally crystallized phases are homogenous and no quench crystals are present in any experiment, suggesting successful equilibrium quench.

Analyses

Experimental run products were analyzed using a Cameca SX-100 electron microprobe at NASA JSC for major element abundances of the glass (liquid) as well as the crystal phases. Analytical conditions were standard for the instrument: 15 kV electron accelerating potential, and focused electron beam of 20 nA current (in a Faraday cup). Analytical standards were synthetic oxides, and raw data were reduced in the Cameca PAP routine. Mass balance calculations were conducted, on the starting glass composition (Table 1) and the crystallizing phases and glass compositions, using the least square computations of the IgPet software (Carr 2000) in order to determine mineral abundances and ensure that no phase was missed during microprobe analysis. All elevated pressure experiments have sum of the least-square residuals <0.3 (for 1 bar experiments, minor Fe and Na loss resulted in higher least-square residuals).

Since small amounts of dissolved water can have large effects on liquidus temperatures and phases (e.g., Médard and Grove 2007; Zeng et al. 1999), micro-FTIR analysis was conducted to determine water content of the experimental glasses. Samples were analyzed using a Nicolet Contiuum FTIR at NASA JSC. Total dissolved water contents were determined from the intensity of the broad band at 3570 cm^{-1} of doubly polished glass wafers. For each sample 512 scans were used to acquire each IR spectrum. Total water concentrations were calculated using the procedures of Dixon et al. (1995) and Mandeville et al. (2002).

EXPERIMENTAL RESULTS

Experimental phase assemblages were determined from 0.1–15.7 kbar. Experimental run products included glass only, olivine + glass, pigeonite + glass, and olivine + pigeonite + glass. Compositional data for all phases and glasses are given in Table 2.

Were the Experiments at Equilibrium?

To assess whether olivine and liquid (glass) in the experiments were at chemical equilibrium, we compared their MgO and FeO contents with literature data believed to represent equilibria. Jones (1984, 1995) showed that equilibrium partition coefficients for Mg and Fe between olivine and melt (e.g., D_{MgO} = [MgO in olivine]/[MgO in melt]) are strongly correlated and so can be used to test for equilibrium (Fig. 1). D_{MgO} and D_{FeO} from these experiments fall close to the equilibrium regression line of Jones (1995), and within its uncertainty. Compared to the regression of Jones (1995), the olivine-melt data here show slightly larger D_{FeO} at a given D_{MgO} (Fig. 1). as do the data of Musselwhite et al. (2006), which also are for high-pressure liquidi of a magnesian Martian composition. Musselwhite et al. (2006) attributed this small difference to the effect of pressure; however there may also be a slight compositional or fO_2 effect. $K^D_{FeO\text{-}MgO} = [X_{FeO}{}^{(Ol)}X_{MgO}{}^{L}]/[X_{MgO}{}^{(Ol)}X_{FeO}{}^{L}]$ was also calculated to assess equilibrium of the crystallizing phases (Table 2). All olivine fall within the expected range for equilibrium (0.3–0.35) suggesting that they are in equilibrium (Roeder and Emslie, 1970). Thus, the run products from the Humphrey experiments are consistent with the attainment of olivine-melt equilibria.

7.7–15.7 kbar Experimental Results

A phase relation diagram which summarizes the results in pressure-temperature space for the experiments conducted on the Humphrey composition is shown in Fig. 2. All experiments below 12 kbar show olivine as the liquidus phase, and crystallize pigeonite + olivine at lower temperatures. Once pigeonite crystallizes, its abundance increases with small decreases in temperature and pigeonite becomes the most abundant phase present. With decreasing temperature the CaO content of the pigeonite increases (Fig. 3). The experiments conducted at 13.7 and 15.7 kbar have pigeonite on the liquidus, and at approximately 12.5 kbar and 1375 °C there is an implied multiple saturation point with both olivine and pigeonite on the liquidus.

2 kbar Experimental Results

The 2 kbar liquidus experiments all contained metallic iron, although the proportion of iron metal decreases with increasing proportion of olivine. We rationalize this by noting that the metallic iron must come from reduction of ferrous iron in the melt, and so that production of iron metal decreases the Fe/Mg of the melt. This, in turn, allows formation of more magnesian olivine, which has greater thermal stability than ferroan iron. Therefore, these experiments are not directly relevant to our study, but do suggest that the fO_2 of the experiments is between the IW buffer and the quartz-iron-

Table 2. Average residual liquid compositions, phase assemblages, and phase compositions.

Temperature (°C)	1400	1385	1385	1378	1350	1350	1333	1333	1380
Pressure (kbar)	15.7	15.7	15.7	13.7	13.7	13.7	13.7	13.7	11.7
Run number	H-20	H-19	H-19	H-10	H-22	H-22	H-11	H-11	H-17
Phase	Glass	Glass	Pigeonite	Glass	Glass	Pigeonite	Glass	Pigeonite	Glass
SiO_2	45.24	44.96	51.63	46.45	45.46	52.40	44.88	50.48	47.02
TiO_2	0.54	0.63	0.11	0.55	0.59	0.08	0.73	0.21	0.55
Al_2O_3	10.95	11.75	4.68	11.03	11.10	3.26	12.97	5.89	11.11
FeO_T	19.36	20.58	16.36	19.48	19.68	15.80	21.02	17.08	19.47
MnO	0.42	0.42	0.48	0.44	0.42	0.44	0.39	0.47	0.42
MgO	10.66	8.97	22.21	10.31	9.75	23.99	6.58	17.95	10.58
CaO	7.78	8.41	4.93	8.01	8.12	3.27	8.38	7.67	8.04
Na_2O	2.43	2.76	0.39	2.30	2.52	0.19	2.84	0.47	2.25
K_2O	0.11	0.13	0.00	0.11	0.11	0.00	0.15	0.01	0.11
P_2O_5	0.63	0.72	0.07	0.60	0.66	0.04	0.78	0.08	0.58
Total	98.12	99.33	100.86	99.28	98.41	99.47	98.72	100.31	100.12
Water (wt%)				0.17			0.11		
$K_D^{FeO-MgO}$			0.32			0.33		0.30	
Phase abun. (wt%)	100	86	14	100	95	5	62	38	100
Phase comp.			$En_{64}Wo_{15}Fs_{22}$			$En_{68}Wo_9Fs_{23}$		$En_{53}Wo_{21}Fs_{26}$	
Temperature (°C)	1370	1370	1365	1365	1350	1350	1350	1325	1325
Pressure (kbar)	11.7	11.7	11.7	11.7	11.7	11.7	11.7	11.7	11.7
Run number	H-14	H-14	H-12	H-12	H-6	H-6	H-6	H-4	H-4
Phase	Glass	Olivine	Glass	Olivine	Glass	Olivine	Pigeonite	Glass	Olivine
SiO_2	46.48	37.66	46.24	37.36	44.90	36.54	51.31	47.08	37.87
TiO_2	0.57	0.01	0.58	0.02	0.59	0.02	0.11	0.61	0.01
Al_2O_3	11.33	0.09	11.12	0.08	11.57	0.08	3.76	11.75	0.10
FeO_T	19.21	25.66	19.54	25.71	19.55	27.48	16.27	19.73	28.20
MnO	0.42	0.46	0.45	0.46	0.43	0.47	0.47	0.40	0.46
MgO	9.93	37.23	9.87	35.46	8.72	34.06	22.53	8.07	34.17
CaO	8.18	0.29	8.13	0.29	8.65	0.34	4.11	8.73	0.32
Na_2O	2.32	0.03	2.28	0.05	2.26	0.03	0.23	2.38	0.05
K_2O	0.12	0.00	0.11	0.01	0.11	0.01	0.00	0.12	0.00
P_2O_5	0.56	0.18	0.58	0.12	0.62	0.12	0.03	0.62	0.34
Total	99.12	101.61	98.89	99.55	97.41	99.14	98.83	99.50	101.53
Water (wt%)			0.12		0.12				
$K_D^{FeO-MgO}$		0.36		0.37		0.36	0.32		0.34
Phase abun. (wt%)	97	3	97	3	89	7	4	87	8
Phase comp.		$Fo_{72}Fa_{28}$		$Fo_{71}Fa_{29}$		$Fo_{69}Fa_{31}$	$En_{65}Wo_{11}Fs_{24}$		$Fo_{68}Fa_{32}$
Temperature (°C)	1325	1362	1345	1345	1325	1325	1307	1307	1307
Pressure (kbar)	11.7	9.7	9.7	9.7	9.7	9.7	9.7	9.7	9.7
Run number	H-4	H-7	H-5	H-5	H-3	H-3	H-1	H-1	H-1
Phase	Pigeonite	Glass	Glass	Olivine	Glass	Olivine	Glass	Olivine	Pigeonite
SiO_2	53.62	44.98	46.01	36.51	45.52	36.71	47.02	36.99	52.80
TiO_2	0.13	0.55	0.60	0.02	0.58	0.00	0.63	0.01	0.12
Al_2O_3	3.75	10.65	11.95	0.06	11.27	0.06	12.54	0.25	2.40
FeO_T	16.94	19.57	18.31	27.32	18.82	27.95	18.92	30.13	17.72
MnO	0.47	0.41	0.39	0.50	0.43	0.51	0.41	0.50	0.48
MgO	21.40	10.65	8.13	34.28	7.91	33.34	6.85	33.30	22.47
CaO	4.98	7.94	8.68	0.30	9.01	0.33	9.38	0.36	4.64
Na_2O	0.26	2.39	2.12	0.04	2.49	0.03	2.63	0.02	0.16
K_2O	0.01	0.10	0.17	0.01	0.13	0.00	0.12	0.00	0.00
P_2O_5	0.09	0.57	0.64	0.23	0.64	0.21	0.70	0.05	0.06
Total	101.64	97.80	96.99	99.27	96.80	99.15	99.21	101.63	100.85
Water (wt%)		0.12	0.09		0.25				
$K_D^{FeO-MgO}$	0.32			0.35		0.35		0.33	0.29
Phase abun. (wt%)	5	100	91	9	89	11	83	11	6
Phase comp.	$En_{59}Wo_{15}Fs_{26}$			$Fo_{69}Fa_{31}$		$Fo_{68}Fa_{32}$		$Fo_{66}Fa_{34}$	$En_{63}Wo_{12}Fs_{25}$

Table 2. *(Continued).* Average residual liquid compositions, phase assemblages, and phase compositions.

Temperature (°C)	1340	1320	1320	1345	1345	1330	1330	1330	1315
Pressure (kbar)	7.7	7.7	7.7	2	2	2	2	2	2
Run number	H-26	H-27	H-27	H-16	H-16	H-15	H-15	H-15	H-13
Phase	Glass	Glass	Olivine	Glass	Fe metal	Glass	Fe metal	Olivine	Glass
SiO_2	46.28	46.85	38.72	50.89	0.06	46.73	0.31	37.43	46.68
TiO_2	0.54	0.61	0.03	0.61	0.04	0.57	0.06	0.03	0.54
Al_2O_3	10.74	11.08	0.32	11.94	0.03	11.03	0.06	0.06	10.98
FeO_T	19.85	19.71	25.55	11.42	120.38	18.11	122.65	22.53	19.31
MnO	0.42	0.39	0.42	0.48	0.05	0.45	0.00	0.42	0.42
MgO	10.70	9.81	35.56	11.79	0.00	10.88	0.01	39.30	10.33
CaO	7.95	8.28	0.47	8.59	0.19	8.39	0.31	0.36	8.00
Na_2O	2.50	2.13	0.06	2.69	0.01	2.42	0.03	0.02	2.25
K_2O	0.11	0.10	0.01	0.12	0.00	0.11	0.01	0.01	0.11
P_2O_5	0.64	0.58	0.31	0.52	0.12	0.60	0.00	0.29	0.54
Total	99.73	99.55	101.45	99.06	120.87	99.30	123.42	100.45	99.15
Water (wt%)									0.10
$K_D^{FeO-MgO}$			0.36					0.34	
Phase abun. (wt%)	100	96	4	90	10	98	2	tr	98
Phase comp.			$Fo_{71}Fa_{29}$					$Fo_{75}Fa_{25}$	
Temperature (°C)	1315	1315	1260	1260	1260	1300	1250	1250	
Pressure (kbar)	2	2	2	2	2	1 bar/FMQ	1 bar/ FMQ	1 bar/ FMQ	
Run number	H-13	H-13	H-31	H-31	H-31	H-21	H-23	H-23	
Phase	Fe metal	Olivine	Glass	Fe metal	Olivine	Glass	Glass	Olivine	
SiO_2	0.03	38.13	47.21	0.04	37.92	46.51	47.57	38.44	
TiO_2	0.01	0.01	0.61	0.01	0.02	0.57	0.61	0.01	
Al_2O_3	0.01	0.08	11.25	0.01	0.09	10.85	11.68	0.05	
FeO_T	120.34	24.00	19.33	113.05	26.75	18.89	18.83	23.36	
MnO	0.00	0.46	0.41	0.02	0.46	0.43	0.42	0.46	
MgO	0.00	37.64	8.71	0.00	35.37	10.86	9.15	39.00	
CaO	0.13	0.33	8.89	0.01	0.36	8.00	8.58	0.30	
Na_2O	0.00	0.01	2.38	0.15	0.03	1.75	2.07	0.01	
K_2O	0.00	0.01	0.12	0.01	0.01	0.08	0.10	0.00	
P_2O_5	2.04	0.34	0.62	0.12	0.16	0.39	0.47	0.02	
Total	122.56	101.01	99.52	113.41	101.16	98.32	99.49	101.67	
Water (wt%)						0.0	0.0	0.0	
$K_D^{FeO-MgO}$		0.34			0.34			0.29	
Phase abun. (wt%)	2	1	92	tr	8	100	94	6	
Phase comp.		$Fo_{73}Fa_{27}$			$Fo_{70}Fa_{30}$			$Fo_{75}Fa_{25}$	
Temperature (°C)	1330	1280	1280	1260	1260	1200	1200		
Pressure/fO_2	1 bar/ IW-1	1 bar/ IW-1	1 bar/ IW-1	1 bar/ IW-1	1 bar/ IW-1	1 bar/ IW-1	1 bar/ IW-1		
Run number	H-37	H-34	H-34	H-35	H-35	H-36	H-36		
Phase	Glass	Glass	Olivine	Glass	Olivine	Glass	Olivine		
SiO_2	46.79	46.56	37.37	48.81	38.73	49.48	38.18		
TiO_2	0.56	0.60	0.01	0.62	0.02	0.68	0.02		
Al_2O_3	10.85	11.17	0.05	11.57	0.11	12.88	0.07		
FeO_T	18.94	19.84	25.60	20.06	26.21	18.12	30.47		
MnO	0.39	0.43	0.44	0.44	0.44	0.41	0.56		
MgO	10.75	9.96	36.59	9.75	36.58	6.75	33.13		
CaO	8.06	8.49	0.24	8.60	0.26	9.52	0.38		
Na_2O	1.76	0.64	0.01	0.49	0.00	2.05	0.01		
K_2O	0.10	0.05	0.00	0.04	0.00	0.10	0.00		
P_2O_5	0.37	0.19	0.03	0.18	0.02	0.55	0.15		
Total	98.56	97.92	100.35	100.57	102.37	100.54	102.99		
Water (wt%)	0.0	0.0	0.0	0.0	0.0	0.0	0.0		
$K_D^{FeO-MgO}$			0.35		0.35		0.34		
Phase abun. (wt%)	100	98	2	95	5	84	16		
Phase comp.			$Fo_{72}Fa_{28}$		$Fo_{70}Fa_{30}$		$Fo_{66}Fa_{34}$		

Components: Fo (forsterite); Fa (fayalite); En (enstatite); Wo (wollastonite); Fs (ferrosilite). tr = trace amounts. FeO_T = total iron (Fe_2O_3 + FeO). $K_D^{FeO-MgO} = [X_{FeO}^{(ol, pig)}X_{MgO}^{L}]/[X_{MgO}^{(Ol,Pig)}X_{FeO}^{L}]$.

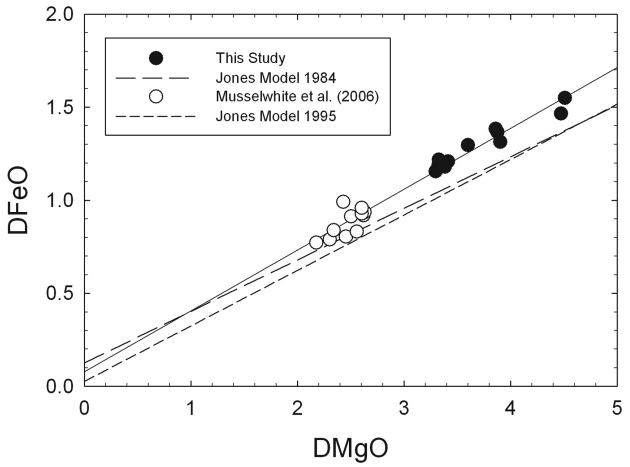

Fig. 1. Cation fraction crystal/melt partition coefficients for Mg (D_{MgO}) and Fe (D_{FeO}) for experimentally produced olivine from this study compared with the experiments from Musselwhite et al. (2006) and the models of Jones (1984, 1995). The solid line is a best-fit regression line for the elevated pressure experiments ($r^2 = 0.96$).

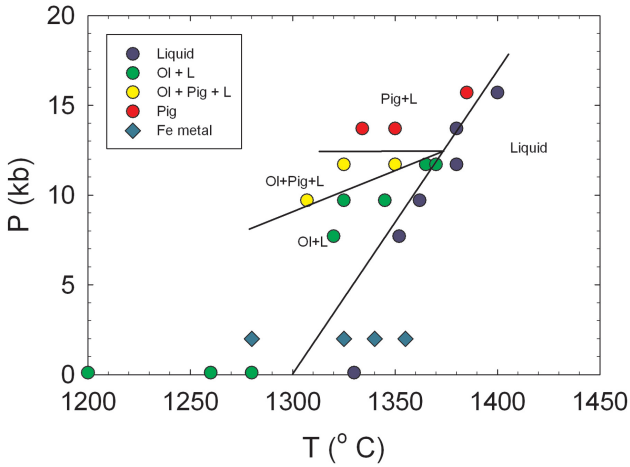

Fig. 2. Experimental determined phase relations for synthetic Humphrey basalt. Blue circles are experiments that contained liquid only, green are olivine and liquid, yellow are olivine, pigeonite, and liquid, and red are pigeonite and liquid. Diamonds are experiments that contained Fe metal, liquid, and olivine.

fayalite buffer (QIF). This is at or below the fO_2 suggested by Holloway et al. (1992) for higher pressure graphite capsule piston-cylinder experiments.

1 bar Experimental Results

Experiments at 1 bar yielded olivine on the liquidus at oxygen fugacities of IW-1 and FMQ. The FMQ results have a lower liquidus temperature than the experiments conducted at IW-1 (Table 2). The experiments conducted at IW-1 agree with the fO_2 suggested by the graphite experiments as well as match the phase relations and projected liquidus of the higher pressure results.

H_2O Content

Dissolved water is an important variable that influences phase assemblages, since it destabilizes feldspars and lowers the liquidus temperature by breaking bridging oxygen linkages in the melt (e.g., Zeng et al. 1999). Therefore, water contents of starting materials and run products were carefully monitored. Analysis of 1 bar experiments revealed 0.0 wt% water, whereas the higher pressure experiments contain 0.1 wt% water. This is relatively anhydrous and should not affect phase relations significantly. However the small amount of water in the high pressure experiments will depress the liquidus temperatures and the truly anhydrous liquidus is at slightly higher temperatures.

COMPARISON WITH PREVIOUS EXPERIMENTAL WORK

Recently Monders et al. (2007) also determined the high-pressure liquidus phase relations of a Humphrey composition, with results rather different from those here. Monders et al. (2007) located the liquidus at approximately 50 °C lower temperature than our results, and also produced orthopyroxene rather than pigeonite pyroxene. To explain these differences, one can point to two differences: water content and experimental procedures.

Water can have a dramatic effect on liquidus location and phase equilibria in basaltic systems, and it seems likely that most of the difference between the results here and those of Monders et al. (2007) relates to water. In the experiments here, water was carefully excluded from the system, and the glasses contain only ~0.1% H_2O (Table 2). However, glasses in the work of Monders et al. (2007) contained ~0.8 wt% bulk H_2O. This difference in water content could reasonably account for ~50°C difference in liquidus temperatures.

Monders et al. (2007) also found that orthopyroxene, not pigeonite, was the liquidus phase at higher pressures. The experimental results here, showing liquidus pigeonite, are consistent with other anhydrous experiments on similar compositions at similar pressures (Nekvasil et al. 2007b; O'Leary et al. 2006) and with MELTS modeling calculations of the anhydrous system (Ghiorso et al. 2002). It is not clear if the liquidus depression caused by the water content of their experiments would affect which pyroxene was produced. However, the previous experiments (Monders et al. 2007) were conducted using a slightly different starting composition (Table 3) than the experiments in this study (i.e., ~1 wt% less FeO, ~0.7 wt% less Na_2O, 0.7 wt% Cr_2O_3) which could have an effect on phase equilibrium. A decrease in iron, which increases the Mg#, in the bulk composition will help stabilize orthopyroxene with respect to pigeonite (e.g., Grove and Juster 1989; Longhi 1991). The addition of chromium to their system helped stabilize chromite to higher temperatures than the olivine and pyroxene thereby

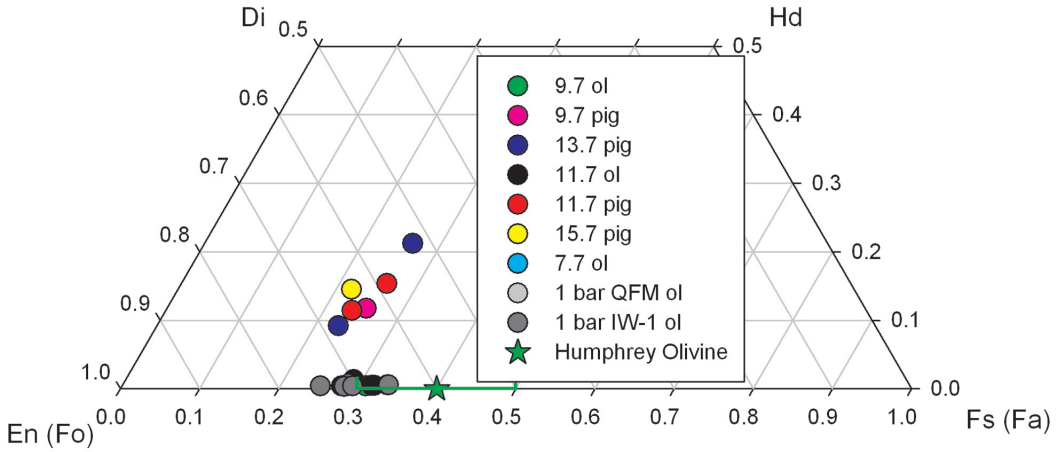

Fig. 3. Compositions of experimentally produced pigeonite (Pig) and olivine (Ol) plotted as QUIlF (Andersen et al. 1993) projections for all pressures produced in this study. The olivine compositions predicted to be in the rock (Morris et al. 2004) are shown by a green star with uncertainty in the measurement (±Fo_{10}; Morris, personal communication).

decreasing the Mg# of the bulk liquid which would again help stabilize orthopyroxene (e.g., Grove and Juster 1989; Longhi 1991). Also, the experiments of Monders et al. (2007) were syntheses at temperature from powders and not crystallization from melt—it is possible that differences in experimental technique could cause discrepancy in phase relations.

The 1 bar experiments of Monders et al. (2007) were conducted at FMQ. These experiments are in agreement with our experiments conducted at FMQ but both sets of experiments have a lower liquidus temperature then our experiments conducted at IW-1. The fO_2 of a crystallizing assemblage can also have an effect on liquidus temperatures with a more oxidizing fO_2 having a lower liquidus temperature.

Table 3. Starting composition compared with starting composition of previous work (normalized to 100%).

wt%	Experimental glass composition	Monders et al. (2007)[a]
SiO_2	45.99	46.85
TiO_2	0.56	0.48
Al_2O_3	10.89	10.69
Cr_2O_3	0.00	0.79
FeO_T	20.01	18.91
MnO	0.42	0.43
MgO	10.89	11.46
CaO	8.12	8.02
Na_2O	2.44	1.77
K_2O	0.10	0.06
P_2O_5	0.58	0.56
Total	100.00	100.00

FeO_T = total iron (Fe_2O_3 + FeO).
[a]Average estimated composition.

DISCUSSION

Is Humphrey a Liquid Composition?

If the Humphrey composition represents a basaltic liquid (and not an altered rock or a crystal accumulate), then the 1-bar crystallization experiments should replicate Humphrey's minerals and their compositions. As Humphrey contains ≤25% olivine crystals, the 1-bar experiments should, after 25% crystallization, contain only glass + olivine of the same composition as that in the rock itself. Figure 3 shows olivine compositions plotted on the pyroxene quadrilateral from all experiments here compared with the Humphrey olivine composition from MER Spirit's Mössbauer. The olivine crystallizing at 1 bar from Humphrey, after about 16% crystallization, is Fo_{66}, which falls in the uncertainty from Mössbauer (~$Fo_{60 \pm 10}$) (Morris et al. 2004; Morris, personal communication). This similarity in olivine compositions, experimental on Earth and analytical on Mars suggests that Humphrey does have the composition of a basaltic liquid. However, without more detailed petrologic data on the exact composition and amount of the olivine and other minerals in the rock, it cannot be definitively concluded that Humphrey represents a liquid composition.

Is Humphrey a Primary Anhydrous Mantle Melt?

If an igneous composition is a primary-mantle melt, there will be a single pressure and temperature at which the liquidus is multiply saturated with the minerals that melted in the mantle to produce the rock. These experimental results show that a rock with the Humphrey composition has an inferred multiple saturation point, with olivine and pigeonite coexisting on the liquidus, at approximately 12.5 kbar and 1375 °C. Notably, the pyroxene crystallizing from Humphrey is pigeonite instead of orthopyroxene. If Humphrey were a primary mantle melt, it would have been in equilibrium with presumed Martian mantle phases (augite, orthopyroxene, olivine) before its ascent to the surface and not with pigeonite (Agee and Draper 2004; Bertka and Holloway 1994a, b).

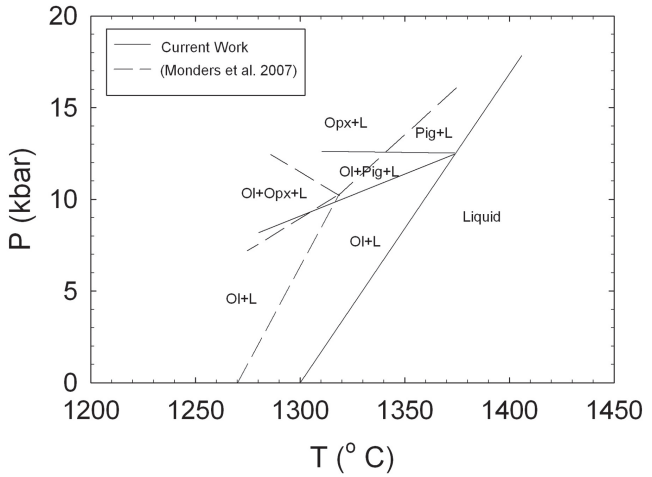

Fig. 4. Experimentally determined phase relations from this study (solid lines) compared with previously published experimental work (dashed lines; Monders et al. 2007). The chromite from Monders et al. (2007) has been disregarded for this comparison since our experiments were conducted Cr-free.

Also, the composition of the first formed olivine is ~Fo_{72}, which is too iron enriched to be in equilibrium with the current proposed Martian mantle compositions (Agee and Draper 2004). This suggests that Humphrey is an evolved magma composition and not an anhydrous pristine mantle melt.

It is not surprising that the Adirondack class basalts have fractionated after their generation in the mantle. Primary mantle-derived melts are not common in terrestrial intra-plate volcanic systems. Terrestrial magmas tend to separate from the source, rise from the mantle into the crust and pond in a sub-volcanic magma chamber where they fractionate. Kiefer (2004) noted gravity evidence for such a cumulate section, suggested to be remnants of a magma chamber, beneath Mars' Syrtis Major volcano.

CONCLUSION

Crystallization experiments on a synthetic Humphrey composition suggest that it could represent a liquid. However without more petrologic data on the phase relations within the rock it is impossible to be certain that Humphrey represents a pure basaltic liquid composition. Elevated pressure crystallization experiments have shown that Humphrey is not a pristine anhydrous partial melt from the Martian mantle, but may instead be a product of lower-pressure magma fractionation.

There is still the possibility that Humphrey is instead a hydrous partial melt of the Martian mantle. Monders et al. (2007) experimentally (with ~0.8 wt% bulk H_2O) produced a mineral assemblage (olivine + orthopyroxene) that is a reasonable proxy for that of a Martian mantle. However, the olivine they produced at 10 kbar is of Fo_{73} composition, which is too iron-rich to have been in equilibrium with proposed Martian mantle compositions (Agee and Draper 2004). Without more detailed petrography of the Humphrey rock and better information on the constitution of the Martian mantle, it is impossible to decisively conclude whether Humphrey is a hydrous melt or a product of low-pressure fractionation. The experiments suggest that the Humphrey composition is an evolved liquid composition produced by low-pressure fractionation and not a direct mantle melt.

Acknowledgments—We are grateful to Lindsay Keller for helping with the FTIR analysis as well as Kevin Righter, Donald H. Lindsley, Richard Morris, Walter S. Kiefer, and John H. Jones for insightful discussions. We thank Dave Draper, Steve Singletary, and an anonymous reviewer for helpful reviews of this manuscript, as well as Cyrena Goodrich for handling this manuscript and her extremely helpful comments. This work was supported by NASA MFR grant no. NNG06GH29G to A. H. Treiman. This is LPI Contribution 1382.

Editorial Handling—Dr. Cyrena Goodrich

REFERENCES

Agee C. B. and Draper D. S. 2004. Experimental constraints on the origin of Martian meteorites and the composition of the Martian mantle. *Earth and Planetary Science Letters* 224:415–429.

Andersen D. J., Lindsley D. H., and Davidson P. M. 1993. QUIlF: A pascal program to assess equilibria among Fe-Mg-Mn-Ti oxides, pyroxenes, olivine, and quartz. *Computers & Geosciences* 19: 1333–1350.

Asimow P. D. and Longhi J. 2004. The significance of multiple saturation points in the context of polybaric near-fractional melting. *Journal of Petrology* 45:2349–2367.

Bertka C. M. and Holloway J. R. 1994a. Anhydrous partial melting of an iron-rich mantle. 1. Subsolidus phase assemblages and partial melting mhase-relations at 10 to 30 kbar. *Contributions to Mineralogy and Petrology* 115:313–322.

Bertka C. M. and Holloway J. R. 1994b. Anhydrous partial melting of an iron-rich mantle. 2. Primary melt compositions at 15 kbar. *Contributions to Mineralogy and Petrology* 115:323–338.

Boyd F. R. and England J. L. 1963. Effect of pressure on melting of diopside, $CaMgSi_2O_6$, and albite, $NaAlSi_3O_8$, in range up to 50 kilobars. *Journal of Geophysical Research* 68:311–323.

Carr M. J. 2000. Igpet for Windows. Terra Softa Inc., Somerset, New Jersey, USA.

Dann J. C., Holzheid A. H., Grove T. L., and Mcsween H. Y. 2001. Phase equilibria of the Shergotty meteorite: Constraints on pre-eruptive water contents of Martian magmas and fractional crystallization under hydrous conditions. *Meteoritics & Planetary Science* 36:793–806.

Danyushevsky L. V. 2001. The effect of small amounts of H_2O on crystallisation of mid-ocean ridge and backarc basin magmas. *Journal of Volcanology and Geothermal Research* 110:265–280.

Dixon J. E., Stolper E. M., and Holloway J. R. 1995. An experimental study of water and carbon dioxide solubilities in mid-ocean ridge basaltic liquids. *Journal of Petrology* 36:1607–1631.

Dyar M. D., Mackwell S. J., Seaman S. J., and Marchand G. J. 2004. Evidence for a wet, reduced Martian interior (abstract #1348). 35th Lunar and Planetary Science Conference. CD-ROM.

Filiberto J. 2008. Experimental constraints on the parental liquid of

the Chassigny meteorite: A possible link between the Chassigny meteorite and a Gusev basalt. *Geochimica et Cosmochimica Acta* 72:690–701.

Gellert R., Rieder R., Bruckner J., Clark B. C., Dreibus G., Klingelhofer G., Lugmair G., Ming D. W., Wänke H., Yen A., Zipfel J., and Squyres S. W. 2006. Alpha Particle X-ray Spectrometer (APXS): Results from Gusev crater and calibration report. *Journal of Geophysical Research-Planets* 111(E2), E02S05, doi:10.1029/2005JE002555.

Ghiorso M. S., Hirschmann M. M., Reiners P. W., and Kress V. C. 2002. The pMELTS: A revision of MELTS for improved calculation of phase relations and major element partitioning related to partial melting of the mantle to 3 GPa. *Geochemistry Geophysics Geosystems* 3:1030, doi:10.1029/2001GC000217.

Greeley R., Foing B. H., McSween H. Y., Neukum G., Pinet P., Van Kan M., Werner S. C., Williams D. W., and Zegers T. E. 2005. Fluid lava flows in Gusev crater, Mars. *Journal of Geophysical Research* 110:E05008.

Grove T. L. and Juster T. C. 1989. Experimental investigations of low-Ca pyroxene stability and olivine-pyroxene-liquid equilibria at 1 atm in natural basaltic and andesitic liquids. *Contributions to Mineralogy and Petrology* 103:287–305.

Holloway J. R., Pan V., and Gudmundsson G. 1992. High-pressure fluid-absent melting experiments in the presence of graphite-oxygen fugacity, ferric ferrous ratio and dissolved CO_2. *European Journal of Mineralogy* 4:105–114.

Jones J. H. 1984. Temperature-independent and pressure-independent correlations of olivine liquid partition-coefficients and their application to trace-element partitioning. *Contributions to Mineralogy and Petrology* 88:126–132.

Jones J. H. 1986. A discussion of isotopic systematics and mineral zoning in the shergottites: Evidence for a 180 m.y. igneous crystallization age. *Geochimica et Cosmochimica Acta* 50:969–977.

Jones J. H. 1995. Experimental trace element partitioning. In *Rock physics and phase relations: A handbook of physical constants*, edited by Ahrens T. J. Washington D.C.: American Geophysical Union. pp. 73–104.

Jones J. H. 2004. The edge of wetness: The case for dry magmatism on Mars (abstract #1798). 35th Lunar and Planetary Science Conference. CD-ROM.

Jones J. H. 2007a. The edge of wetness: The case for dry magmatism on Mars, II (abstract #2006). Workshop on Water in Planetary Basalts. CD-ROM.

Jones J. H. 2007b. The shergottites are young. *Meteoritics & Planetary Science* 42:5194.

Jurewicz A. J. G., Williams R. J., Le L., Wagstaff J., Lofgren G., Lanier A., Carter W., and Roshko A. 1993. Technical update: Johnson Space Center system using a solid electrolytic cell in a remote location to measure oxygen fugacities in CO/CO_2 controlled-atmosphere furnaces. NASA Technical Memoradum #104774. Washington, D.C.: National Aeronautics and Space Administration. 40 p.

Kiefer W. S. 2004. Gravity evidence for an extinct magma chamber beneath Syrtis Major, Mars: A look at the magmatic plumbing system. *Earth and Planetary Science Letters* 222:349–361.

Leshin L. A., Epstein S., and Stolper E. M. 1996. Hydrogen isotope geochemistry of SNC meteorites. *Geochimica et Cosmochimica Acta* 60:2635–2650.

Longhi J. 1991. Comparative liquidus equilibria of hypersthene-normative basalts at low pressure. *American Mineralogist* 76: 785–800.

Mandeville C. W., Webster J. D., Rutherford M. J., Taylor B. E., Timbal A., and Faure K. 2002. Determination of molar absorptivities in infrared absorption bands of H_2O in andesitic glasses. *American Mineralogist* 87:813–821.

McCoy T. J. and Lofgren G. E. 1999. Crystallization of the Zagami shergottite: An experimental study. *Earth and Planetary Science Letters* 173:397–411.

McSween H. Y. 2002. The rocks of Mars, from far and near. *Meteoritics & Planetary Science* 37:7–25.

McSween H. Y., Wyatt M. B., Gellert R., Bell J. F., Morris R. V., Herkenhoff K. E., Crumpler L. S., Milam K. A., Stockstill K. R., Tornabene L. L., Arvidson R. E., Bartlett P., Blaney D., Cabrol N. A., Christensen P. R., Clark B. C., Crisp J. A., Des Marais D. J., Economou T., Farmer J. D., Farrand W., Ghosh A., Golombek M., Gorevan S., Greeley R., Hamilton V. E., Johnson J. R., Joliff B. L., Klingelhöfer G., Knudson A. T., McLennan S., Ming D., Moersch J. E., Rieder R., Ruff S. W., Schröder C., De Souza P. A., Squyres S. W., Wänke H., Wang A., Yen A., and Zipfel J. 2006. Characterization and petrologic interpretation of olivine-rich basalts at Gusev crater, Mars. *Journal of Geophysical Research-Planets* 111(E2): EO2510, doi:1029/2005E02477.

Médard E. and Grove T. 2007. The effect of H_2O on the olivine liquidus of basaltic melts: experiments and thermodynamic models. *Contributions to Mineralogy and Petrology* 155:417–432.

Médard E. and Grove T. L. 2006. Early hydrous melting and degassing of the Martian interior. *Journal of Geophysical Research* 111:E11003.

Monders A. G., Médard E., and Grove T. L. 2007. Phase equilibrium investigations of the Adirondack class basalts from the Gusev plains, Gusev crater, Mars. *Meteoritics & Planetary Science* 42: 131–148.

Morris R. V., Klingelhofer G., Bernhardt B., Schroder C., Rodionov D. S., De Souza P. A., Yen A., Gellert R., Evlanov E. N., Foh J., Kankeleit E., Gutlich P., Ming D. W., Renz F., Wdowiak T., Squyres S. W., and Arvidson R. E. 2004. Mineralogy at Gusev crater from the Mössbauer spectrometer on the Spirit rover. *Science* 305:833–836.

Musselwhite D. S., Dalton H. A., Kiefer W. S., and Treiman A. H. 2006. Experimental petrology of the basaltic shergottite Yamato-980459: Implications for the thermal structure of the Martian mantle. *Meteoritics & Planetary Science* 41:1271–1290.

Nekvasil H., Dondolini A., Horn J., Filiberto J., Long H., and Lindsley D. H. 2004. The origin and evolution of silica-saturated alkalic suites: An experimental study. *Journal of Petrology* 45: 693–721.

Nekvasil H., Filiberto J., McCubbin F. M. and Lindsley D. H. 2007a. Alkalic parental magmas for the chassignites? *Meteoritics & Planetary Science* 42:979–992.

Nekvasil H., McCubbin F. M., O'Leary M. C., and Lindsley D. H. 2007b. Exploring possible petrogenetic links between Gusev picrobasalts, alkalic rocks from the Columbia Hills, and the chassignites (abstract #1312). 38th Lunar and Planetary Science Conference. CD-ROM.

Nyquist L. E., Bogard D. D., Shih C. Y., Greshake A., Stöffler D., and Eugster O. 2001. Ages and geologic histories of martian meteorites. *Space Science Reviews* 96:105–164.

O'Leary M. C., McCubbin F. M., Nekvasil H., Beavon L. J., and Lindsley D. H. 2006. Liquid evolution during experimental crystallization of the Gusev basalt, Humphrey, at 10 kbar. *Geological Society of America Abstracts with Programs* 38:307.

Onuma K. and Tohara T. 1983. Effect of chromium on phase relations in the join forsterite-anorthite-diopside in air at 1 atm. *Contributions to Mineralogy and Petrology* 84:174–181.

Roeder P. L. and Emslie R. F. 1970. Olivine-liquid equilibrium. *Contributions to Mineralogy and Petrology* 29(4):275–289.

Treiman A. H. 2005. The nakhlite meteorites: Augite-rich igneous rocks from Mars. *Chemie der Erde-Geochemistry* 65:203–270.
Watson L. L., Hutcheon I. D., Epstein S., and Stolper E. M. 1994. Water on Mars: Clues from deuterium/hydrogen and water contents of hydrous phases in SNC meteorites. *Science* 265:86–90.
Williams D. W. and Kennedy G. C. 1969. Melting curve of diopside to 50 kilobars. *Journal of Geophysical Research* 74:4359.
Yoder S. Y. J. 1952. Change of melting point of diopside with pressure. *Journal of Geology* 60:364–374.
Zeng Q., Nekvasil H., and Grey C. P. 1999. Proton environments in hydrous aluminosilicate glasses: A H-1 MAS, H-1/Al-27, and H-1/Na-23 TRAPDOR NMR study. *Journal of Physical Chemistry B* 103:7406–7415.

APPENDIX

Piston Cylinder Pressure Calibration Data

The pressure was calibrated in the same manner as Musselwhite et al. (2006) using the melting point of diopside (Yoder 1952; Boyd and England 1963; Williams and Kennedy 1969). An experimental assembly identical to those used in the Humphrey experiments was employed. Synthetic diopside glass powder was loaded into a graphite capsule, and dried at 150 °C for at least 12 h. Experiments were conducted in an identical manner to those used in the Humphrey experiments. Polished thin sections were made of the run products to optically investigate if there were any crystalline phases. The run temperatures and pressures from this work as well as from Musselwhite et al. (2006) are plotted in Fig. A1 and fitted with a melting point curve, for reference the diopside melting point curve is also plotted (Yoder 1952; Williams and Kennedy 1969). For the nominally 4 kbar experiments the experiments of Yoder (1952) were used as a reference set and give a negative 2.0 kb correction. For the higher pressure data there is a 0.3 kbar offset between the experiments and the reference curve from Williams and Kennedy (1969).

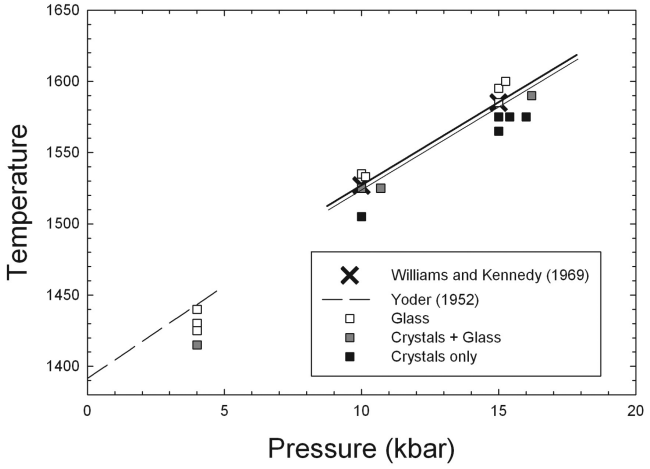

Fig. A1. Results from diopside melting point experiments from this study as well as Musselwhite et al. (2006). The dashed line is from Yoder (1952) and the solid line is from Williams and Kennedy (1969). At low pressure there is a 2 kbar offset between our experiments and those of Yoder (1952) and an even greater offset between our experiments and those of Williams and Kennedy (1969). At pressures greater than 10 kbar there is a 0.3 kbar offset.